Definition and Characterization of the Short αA-Conotoxins: A Single Residue Determines Dissociation Kinetics from the Fetal Muscle Nicotinic Acetylcholine Receptor†

Russell W. Teichert,*,‡,§ Estuardo López-Vera,‡,§ Jozsef Gulyas,|| Maren Watkins,⊥ Jean Rivier,|| and Baldomero M. Olivera‡

Departments of Biology and Pathology, University of Utah, Salt Lake City, Utah, 84112, and Clayton Foundation Laboratories for Peptide Biology, Salk Institute, La Jolla, California 92037

Received October 4, 2005; Revised Manuscript Received November 29, 2005

ABSTRACT: We report the definition and characterization of a conotoxin subfamily, designated the short αA-conotoxins (αA_S) and demonstrate that all of these share the unique property of selectively antagonizing the fetal subtype of the mammalian neuromuscular nicotinic acetylcholine receptor (nAChR). We have characterized newly identified αA_S-conotoxins from *Conus pergrandis* and have conducted a more detailed characterization of αA-conotoxins previously reported from additional *Conus* species. Among the results, the characterization of the short αA-conotoxins revealed diverse kinetics of a block of the fetal muscle nAChR, particularly in dissociation rates. The structure−function relationships of native αA_S-conotoxins and some analogues revealed a single amino acid locus (alternatively either His or Pro in native peptides) that is a critical determinant of the dissociation kinetics. The unprecedented binding selectivity for the fetal muscle nAChR, coupled with the kinetic diversity, should make αA_S-conotoxins useful ligands for a diverse set of studies. The rapidly reversible peptides may be most suitable for electrophysiological studies, while the relatively irreversible peptides should be most useful for binding and localization studies.

In mammals, there is a well-characterized developmental switch in the protein subunits that comprise the nicotinic acetylcholine receptor (nAChR)[1] at the neuromuscular junction. The fetal subtype consists of $\alpha 1\beta 1\gamma\delta$ subunits. The γ subunit is exchanged for an ϵ subunit to create the adult receptor subtype ($\alpha 1\beta 1\epsilon\delta$ subunits) (*1*−*3*). Although it is called a receptor, the nAChR is actually a ligand-gated ion channel that becomes permeable to cations upon the interaction of the neurotransmitter acetylcholine with two binding sites on the α/δ and α/γ subunit interfaces of the fetal receptor or the α/δ and α/ϵ subunit interfaces of the adult receptor. The flow of cations through the nAChR ion channel results in depolarization of the postsynaptic membrane, ultimately resulting in muscle contraction.

Numerous peptide toxins from venomous animals have been shown to antagonize the nAChR at the neuromuscular junction for the paralysis of prey, typically through competitive inhibition of acetylcholine binding at one or both receptor interfaces. Notable among such paralytic nAChR antagonists are the snake α-neurotoxins sharing a three-finger fold, such as α-bungarotoxin (*4*), and a subset of the conotoxins, which are small, disulfide-rich peptides from the venoms of marine cone snails (see refs *5* and *6* for conotoxin reviews). Until recently, no pharmacological agent had been shown to selectively block the fetal nAChR subtype. Such specificity requires preferential antagonism of the α/γ interface of the fetal receptor over both the α/δ and α/ϵ interfaces of the adult muscle nAChR. We previously reported the characterization of a peptide toxin from the venom of the marine cone snail, *Conus obscurus*, that inhibits the fetal subtype of the mammalian muscle nAChR with both high affinity and unprecedented specificity (*7*). Because of its unique specificity, this peptide, αA-conotoxin OIVB (αA-OIVB), has generated interest among neuroscientists as a research tool, with possible additional application in diagnostics and/or therapeutics as described previously (*7*). Here, we report the definition and characterization of a subfamily of conotoxins, the short αA-conotoxins (αA_S), which includes αA-OIVB.

The purification and partial characterization of one of the αA_S-conotoxins, αA-conotoxin OIVA (αA-OIVA), were reported previously; it was formerly identified as a low-

† This work was supported by National Institutes of Health Program Project GM 48677.

* To whom correspondence should be addressed: Department of Biology, University of Utah, 257 South 1400 East, Salt Lake City, UT 84112. Telephone: 801-581-8370. Fax: 801-585-5010. E-mail: teichert@biology.utah.edu.

‡ Department of Biology, University of Utah.

§ These authors contributed equally to this work.

|| Salk Institute.

⊥ Department of Pathology, University of Utah.

[1] Abbreviations: nAChR, nicotinic acetylcholine receptor; αA, αA-conotoxin; αA_S, short αA-conotoxin; αA_L, long αA-conotoxin; UTR, untranslated region; Boc, *tert*-butoxycarbonyl; DIC, *N*,*N*′-diisopropylcarbodiimide; HOBt, 1-hydroxybenzotriazole; TBTU, 2-(1*H*-benzotriazol-yl)-1,1,3,3-tetramethyluronium tetrafluoroborate; DIPEA, diisopropylethylamine; TFA, trifluoroacetic acid; DCM, dichloromethane; HF, hydrogen fluoride; HPLC, high-performance liquid chromatography; MS, mass spectrometry; TEAP, triethylammonium phosphate; CZE, capillary zone electrophoresis; MALDI−MS, matrix-assisted laser desorption ionization−mass spectrometry; CMV, cytomegalovirus; BSA, bovine serum albumin; ACh, acetylcholine; SEM, standard error of the mean; CI, confidence interval.

10.1021/bi052016d CCC: $33.50 © 2006 American Chemical Society
Published on Web 01/06/2006

affinity inhibitor of the adult subtype of the mammalian muscle nAChR (*8*). Additionally, we have characterized two conotoxins from *Conus pergrandis* that exhibit considerable sequence similarity with αA-OIVA and OIVB. Characterization of these peptides firmly establishes that members of the subfamily comprise a group of nAChR inhibitors that are fetal-muscle-subtype-specific but with diverse kinetics of block.

Members of the αA_S-conotoxin subfamily are distinguished from the original αA-conotoxins characterized from *Conus purpurascens* and *C. ermineus* (*9*, *10*), now designated the long αA-conotoxin (αA_L) subfamily by both pharmacological and biochemical criteria. The αA_L-conotoxins are high-affinity antagonists of both the fetal and adult mammalian muscle nAChRs, in contrast to the selectivity of the αA_S-conotoxins for the fetal subtype. The characterization of the native αA_S-conotoxins and some analogues has led to the identification of a key amino acid residue in αA_S peptides that is a critical determinant for a slow versus fast off rate from the fetal muscle nAChR.

MATERIALS AND METHODS

Molecular Cloning of Genes Encoding C. pergrandis Peptides. Genomic DNA was prepared from 50 mg of *C. pergrandis* tissue using the Gentra PUREGENE DNA Isolation Kit (Gentra Systems, Minneapolis, MN), according to the standard protocol of the manufacturer. Genomic DNA from *C. pergrandis* was used as a template for the polymerase chain reaction (PCR), with oligonucleotide primers corresponding to the conserved intron and 3′ untranslated region (UTR) sequences of A-superfamily conotoxin prepropeptides. The resulting PCR products were purified using the High Pure PCR Product Purification Kit (Roche Diagnostics, Indianapolis, IN), following the suggested protocol of the manufacturer. The eluted DNA fragments were ligated to the pAMP1 vector, and the resulting products were transformed into competent DH5α cells, using the CloneAmp pAMP System for Rapid Cloning of Amplification Products (Life Technologies/Gibco BRL, Grand Island, NY), following suggested protocols of the manufacturer. The nucleic acid sequences of the resulting αA-toxin-encoding clones were determined according to the standard protocol for automated sequencing.

Purification of αA-Conotoxins OIVA and OIVB. The purifications of αA-conotoxins OIVA and OIVB were described previously (*7*, *8*).

Total Synthesis of αA-Conotoxins OIVA and OIVB. The total syntheses of αA-conotoxins OIVA and OIVB were described previously (*7*, *8*)

Synthesis of αA-OIVA Analogues. Analogues of αA-OIVA were synthesized on a methylbenzhydryl resin (MBHA resin) (2.0 g and a substitution of 0.20 mmol of amino function/g) using the *tert*-butoxycarbonyl (Boc) protocol [3-fold excess of amino acid derivatives, *N*,*N*′-diisopropylcarbodiimide (DIC), DIC/1-hydroxybenzotriazole (HOBt), or 2-(1*H*-benzotriazol-yl)-1,1,3,3-tetramethyluronium tetrafluoroborate (TBTU)/diisopropylethylamine (DIPEA)/HOBt mediated 30 min couplings and 10 min 60% TFA in dichloromethane (DCM) deblocking]. We used the Kaiser test to monitor coupling efficiencies in all cases, except after hydroxyproline, when we used the tetrachloro-1,4-benzoquinone-acetaldehyde method (*11*). The weight of the dry peptide resin increased an average of 80%.

Cleavage and deprotection was performed using hydrogen fluoride (HF) and scavengers (anisole, dimethyl sulfide) for 1 h at 0 °C. After HF evaporation, peptide and resin were washed with a mixture of diethyl-ether−mercaptoethanol (99:1, v/v). The crude peptide was extracted with a solvent mixture [0.1% trifluoroacetic acid (TFA), 60% acetonitrile−water, v/v]. The extract was diluted 10-fold with water and immediately loaded to a preparative high-performance liquid chromatography (HPLC) cartridge.

Equipment. Shimadzu SCL-10A system controller, Shimadzu 10A-VP UV/vis detector, Shimadzu LC-8A preparative HPLC pumps, and Waters 1000 PrepPAK radial compression module. Cartridge: 50 × 300 mm, C_{18} (15−20 μm particle size, 300 Å pore size).

Conditions. Detection, 220 nm; flow, 100 mL/min; gradient, 5−100% B in 95 min.

Eluents. A = 0.1% TFA−water, and B = 0.1% TFA−60% acetonitrile−water.

Fractions of each peptide were analyzed by HPLC (isocratic conditions that varied between 11 and 14% acetonitrile for the various compounds), checked using mass spectrometry (MS) for identity, pooled, and kept at 4 °C for folding.

Folding of Synthetic αA-OIVA Analogues. Solution A consisted of the pooled, reduced, and purified peptide solution, which was purged with argon. Solution B consisted of water (300 mL), acetonitrile (100 mL), ammonium carbonate (9.6 g), EDTA (100 mg), cysteine−hydrochloride (250 mg), and cystine (250 mg). Solution A was added to the argon-purged solution B. The pH of the mixed solution was adjusted to 8.2 with 20% aqueous acetic acid solution. The mixture was stirred with a Teflon-coated magnetic bar (slow speed) at room temperature under a slow stream of argon. The folding was followed by analytical HPLC. The reaction was stopped after 4 h by addition of pure TFA to acidify the reaction mixture to pH 2.5. The acetonitrile was removed in a vacuum evaporator (bath at 25 °C).

Purification of Synthetic αA-OIVA Analogues. The aqueous solution was loaded to a preparative HPLC equilibrated with triethylammonium phosphate (TEAP) 2.25 buffer (A = 60 mM TEAP, and B = 60% acetonitrile in A). Between 2 and 4 fractions were obtained by HPLC purification from each oxidative folding reaction. The fraction that eluted last from the reverse-phase HPLC column, which was also the most hydrophobic peptide isomer, in each case, was the correctly folded peptide. This was consistent with the prior observation that the native folded αA-OIVA was more hydrophobic than the fully reduced peptide or any partially reduced isomers (*8*). The main component among the most hydrophobic moieties (checked for purity using HPLC) was collected as well as a pool of all side fractions representing misfolded peptides with correct masses. The acetonitrile was removed under vacuum, and the remaining solutions of the desired fractions were desalted using a 0.1% TFA/acetonitrile gradient on preparative HPLC.

Synthesis, Purification, and Characterization of αA-PeIVA and PeIVB. The strategy and protocols for the synthesis, purification, and characterization of αA-PeIVA and αA-PeIVB was identical to those used for the synthesis and purification of αA-OIVA and analogues as described above with one significant difference: a Merrifield resin with a

Table 1: Analytical Data from the Synthesis of Novel Peptides

synthetic peptide	HPLC[a]	CZE[b]	mass calculated[c]	mass found[d]	yield[e]
αA-OIVA[H10P]	85	94	1807.64	1807.79	45.0
αA-OIVB[K15N,N16K]	94	95	1847.65	1847.62	53.3
αA-OIVA[K15N]	99	99	1833.60	1833.67	60.2
αA-OIVA[K15R]	96	90	1875.66	1875.57	25.2
αA-PeIVA	95	97	1791.61	1791.40	75.3
αA-PeIVB	99	90	1805.63	1805.51	86.7

[a] Percentage purity determined by HPLC using buffer system A (TEAP at pH 2.30) and buffer system B (60% CH_3CN/40% A) under gradient conditions (30−80% B over 50 min), at a flow rate of 0.2 mL/min on a Vydac C_{18} column (0.21 × 15 cm, 5 μm particle size, 300 Å pore size). Detection at 214 nm. [b] Percentage of purity determined by capillary zone electrophoresis (CZE) using a Beckman Coulter P/ACE System 2050; field strength of 15 kV at 30 °C; buffer, 100 mM sodium phosphate (85:15 H_2O/CH_3CN) at pH 2.50; on an Agilent μSil bare fused-silica capillary (75 μm i.d. × 40 cm length); detection at 214 nm. [c,d] Mass spectra matrix-assisted laser desorption ionization−mass spectrometry (MALDI−MS) were measured on an ABI-Voyager DESTR instrument using a saturated solution of α-cyano-4-hydroxycinnamic acid in 0.3% TFA and 50% acetonitrile as the matrix. The calculated $[M + H]^+$ of the monoisotope compared with the observed $[M + H]^+$ monoisotopic mass. [e] The yield is in milligrams of final product starting with 2 g of MBHA resin and a substitution of 0.20 mmol of amino function per gram.

substitution of 0.37 mmol/g was used to gain the free carboxylic C terminus after HF cleavage.

Analytical Data. Analytical data for all novel peptides are given in Table 1.

Amino Acid Analysis. Aliquots of all peptides were quantified by amino acid analysis to ensure accuracy of values reported in the Results. Dr. Dennis Winge of the University of Utah conducted the amino acid analysis.

Biological Assays. Intramuscular (i.m.) injections of goldfish and intraperitoneal (i.p.) injections of mice were performed as described previously (*7*, *8*)

Electrophysiology. Plasmid DNA from the cytomegalovirus (CMV)-based pRBG4 vector encoding mouse muscle nAChR subunits (a kind gift from Dr. Steven M. Sine, Mayo Clinic College of Medicine), was prepared and injected into the nucleus of *Xenopus* oocytes. For all other cloned receptors tested, cRNA that encoded receptor subunits was prepared and injected into *Xenopus* oocytes as described previously (*12*). Oocytes were injected 1−2 days after harvesting and used for voltage-clamp recording 1−8 days after injection.

Voltage-clamp recording was done as described in detail previously (*12*). In all cases, oocytes were clamped at −70 mV with a two-electrode system and gravity-perfused with ND96 containing 1 μM atropine to block endogenous muscarinic acetylcholine receptors and 0.1 or 0.2 mg/mL bovine serum albumin (BSA) to reduce nonspecific adsorption of toxin. ND96 consisted of 96 mM NaCl, 2.0 mM KCl, 1.8 mM $CaCl_2$, 1.0 mM $MgCl_2$, and 5 mM HEPES (pH 7.1−7.5). Acetylcholine (ACh)-gated currents were elicited with 1−10 μM ACh for the neuromuscular nAChR subtypes ($\alpha1\beta1\epsilon\delta$ or $\alpha1\beta1\gamma\delta$ subunits), 200 μM ACh for the human α7 nAChR subtype, and 100 μM ACh for all other neuronal nAChR subtypes. For the mouse 5-HT_3 testing, currents were elicited with 3 μM serotonin. The 1 μM concentration of ACh used for the muscle nAChR is significantly lower than the EC_{50} concentration. As a result of high expression levels of muscle nAChR, 1 μM ACh was typically used because, at higher concentrations of ACh, the currents were often too large for voltage-clamping. However, ACh concentrations as high as 100 μM did not appear to affect the current block by the toxins because ACh was applied so briefly that little competition could take place between Ach and toxin, given the off rates of the toxins. A 1-s pulse of ACh or serotonin was applied at a frequency of once per 1 min for all static bath applications of toxin. For toxin perfusion experiments, ACh was applied either at a frequency of once per 1 min or once per 2 min.

We used a distributor valve (SmartValve, Cavro Scientific Instruments, Sunnyvale, CA) and a series of three-way solenoid valves (Neptune Research, Northboro, MA) to switch the perfusion medium between ND96 with or without toxin or ACh. A virtual instrument homemade by Dr. Doju Yoshikami of the University of Utah automated the valve control and data acquisition. All recordings were conducted at room temperature.

In most cases, we tested a given conotoxin concentration against a particular receptor by applying the peptide to an oocyte expressing the receptor in a static bath (30 μL). A predetermined concentration of peptide was allowed to equilibrate with the receptors in the static bath for 5 min prior to pulsing with ACh or serotonin. To establish dose−

Chart 1

C C G V P N A A **C** H P **C** V **C** T G K **C**
TGC TGT GGT GTT CCC AAT GCT GCC **TGT** CAT CCT **TGC** GTA **TGT** ACT GGA AAA **TGC**

C C G I P N A A **C** H P **C** V **C** T G K **C**
TGC TGT GGT ATT CCC AAT GCT GCC **TGT** CAT CCT **TGC** GTA **TGT** ACT GGA AAA **TGC**

Table 2: Categorization of Short and Long αA-Conotoxins

conotoxin	amino acid sequence
short α**A-conotoxins**	inhibit fetal muscle nAChR selectively
αA-OIVB	**CC**GVONAA**C**PO**C**V**C**NKT**C**G#
αA-OIVA	**CC**GVONAA**C**HO**C**V**C**KNT**C**#
αA-PeIVA	**CC**GVONAA**C**HO**C**V**C**TGK**C**
αA-PeIVB	**CC**GIONAA**C**HO**C**V**C**TGK**C**
long α**A-conotoxins**	high-affinity antagonists of fetal and adult muscle nAChR
αA-EIVA	G**CC**GPYONAA**C**HO**C**G**C**KVGROOY**C**DROSGG#
αA-EIVB	G**CC**GKYONAA**C**HO**C**G**C**TVGROOY**C**DROSGG#
αA-PIVA	G**CC**GSYONAA**C**HO**CSC**KDROSY**C**GQ#

[a] O = hydroxyproline. # = amidation.

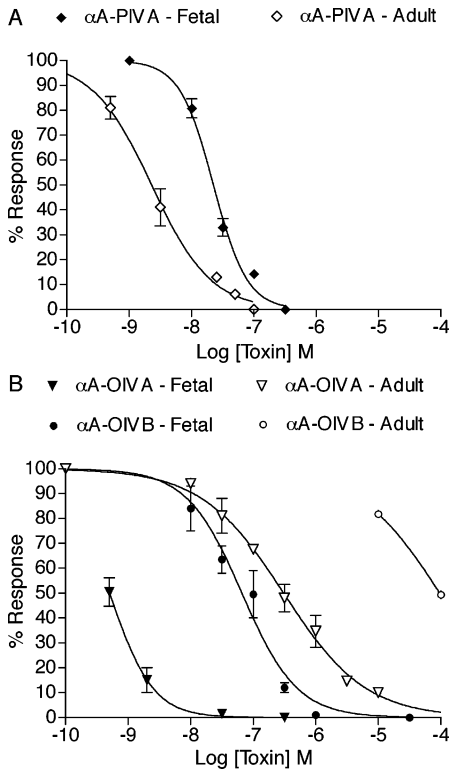

FIGURE 1: αA-Conotoxin PIVA is a high-affinity inhibitor of both the fetal and adult subtypes of the mouse muscle nAChR, in contrast to αA-conotoxins OIVA and OIVB, which are both selective inhibitors of the fetal subtype of the mouse muscle nAChR. *Xenopus* oocytes expressing clones of either the mouse fetal ($\alpha 1\beta 1\gamma\delta$ subunits) or adult ($\alpha 1\beta 1\epsilon\delta$ subunits) muscle nAChR were voltage-clamped at −70 mV. The oocytes were pulsed with ACh once per 1 min to elicit currents and establish the baseline current amplitude, which then served as a control. With the exception of the αA-OIVA block of the fetal muscle nAChR, in all other cases, toxin was applied to oocytes in a static bath at a given concentration and allowed to equilibrate with receptors for 5 min. In the particular case of the αA-OIVA block of the fetal subtype, the kinetics of the block were very slow; consequently, only a partial dose−response curve was obtained by perfusion of various concentrations of toxin over the oocyte until currents reached equilibrium as demonstrated in Figure 3. Dose−response curves were generated by plotting the current amplitude after toxin application as a percentage of the current amplitude prior to toxin application (% response) [$n = 3$ for each toxin concentration; error bars = ± standard error of the mean (SEM)]. (A) αA-PIVA inhibited both the fetal and adult mouse muscle nAChRs with high affinity: IC_{50} for adult subtype = 2.3 nM [1.8−3.0 nM, 95% confidence interval (CI)]; IC_{50} for fetal subtype = 22 nM (20−26 nM, 95% CI). It is possible that the lowest concentrations of αA-PIVA did not reach equilibrium with the fetal receptor within 5 min, resulting in a steeper dose−response curve than expected. (B) αA-OIVA block of the fetal muscle nAChR, $IC_{50} = 0.51$ nM (0.40−0.64 nM, 95% CI). αA-OIVA block of the adult muscle nAChR, $IC_{50} = 310$ nM (240−390 nM, 95% CI). αA-OIVB block of the fetal muscle nAChR, $IC_{50} = 66$ nM (48−92 nM, 95% CI). αA-OIVB block of the adult muscle nAChR, $IC_{50} = 96\,000$ nM (81 000−110 000 nM, 95% CI).

response curves and IC_{50} values, a range of conotoxin concentrations were tested sequentially on an oocyte. This procedure was repeated on three different oocytes for each peptide concentration. To conclude that a peptide did not target a particular receptor, the peptide was tested at a minimum concentration of 10 μM on at least two different oocytes expressing that specific receptor.

In addition to the static-bath applications of the toxin, some dose−response curves and kinetic parameters were determined by perfusion of toxin over oocytes heterologously expressing receptors. This method was employed in cases where the kinetics of the block were particularly slow. A specific concentration of toxin was applied to an oocyte expressing the fetal muscle nAChR by gravity perfusion of the toxin dissolved in ND96 buffer, also containing 0.1 or 0.2 mg/mL BSA and 1 μM atropine. The perfusion continued until the peak amplitude of the elicited currents reached a steady state, at which time the perfusion of toxin changed to a higher concentration to establish a dose−response curve. After a nearly complete block of elicited currents was achieved, the perfusion medium was converted to ND96 containing 0.1 or 0.2 mg/mL BSA and 1 μM atropine, without toxin, to allow the toxin to wash out. Dose−response curves and kinetic data were established after perfusion of toxin over at least three oocytes with reasonably stable currents.

The kinetic− and dose−response curves were generated with Prism software (GraphPad Software, Inc., San Diego, CA). Dose−response curves were fit to the equation: % response = $100/\{1 + ([\text{toxin}]/IC_{50})^{n_H}\}$, where n_H is the Hill coefficient. Kinetic parameters were obtained by a nonlinear

Table 3: IC_{50} Values of αA-Conotoxins for the Fetal versus Adult Subtypes of the Mouse Muscle NAChR[a]

conotoxin	fetal muscle nAChR IC_{50} (nM)	adult muscle nAChR IC_{50} (nM)
αA-OIVA	0.51 (0.40−0.64)	310 (240−390)
αA-OIVB	66 (48−92)	96 000 (81 000−110 000)
αA-PeIVA	<5*	4000 (3800−4200)
αA-PIVA	22 (20−26)	2.3 (1.8−3.0)

[a] Values in parentheses are the 95% CI. (*) αA-PeIVA (5 nM) blocked ~90% of elicited currents. A complete dose−response curve was not generated for αA-PeIVA. However, it is evident that it shares the selectivity for the fetal subtype with the rest of the short αA-conotoxins.

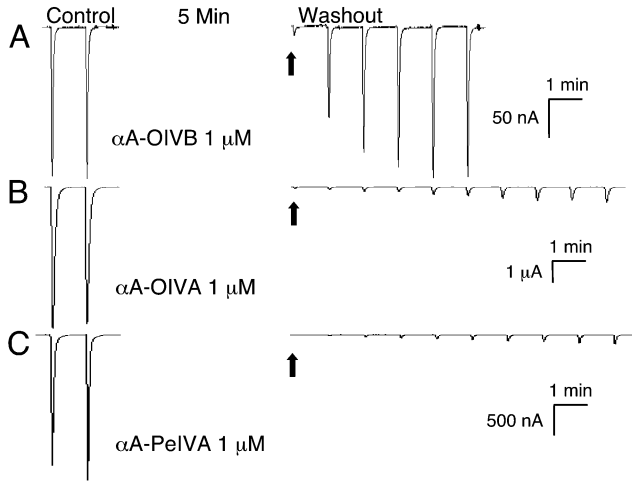

FIGURE 2: αA-Conotoxins OIVA, OIVB, and PeIVA all antagonize the mouse fetal muscle nAChR with high affinity but distinct kinetics. *Xenopus* oocytes heterologously expressing the mouse fetal muscle nAChR were voltage-clamped. Toxin was applied to oocytes in a static bath at a final concentration of 1 μM. Arrows indicate the first currents elicited after the 5 min of toxin equilibration. (A) αA-OIVB (1 μM) blocked the elicited currents nearly completely, and the toxin dissociated rapidly from the receptor. (B) αA-OIVA (1 μM) blocked the elicited currents completely, and the toxin dissociated very slowly from the receptor. (C) αA-PeIVA (1 μM) blocked the elicited currents completely, and the toxin dissociated very slowly from the receptor.

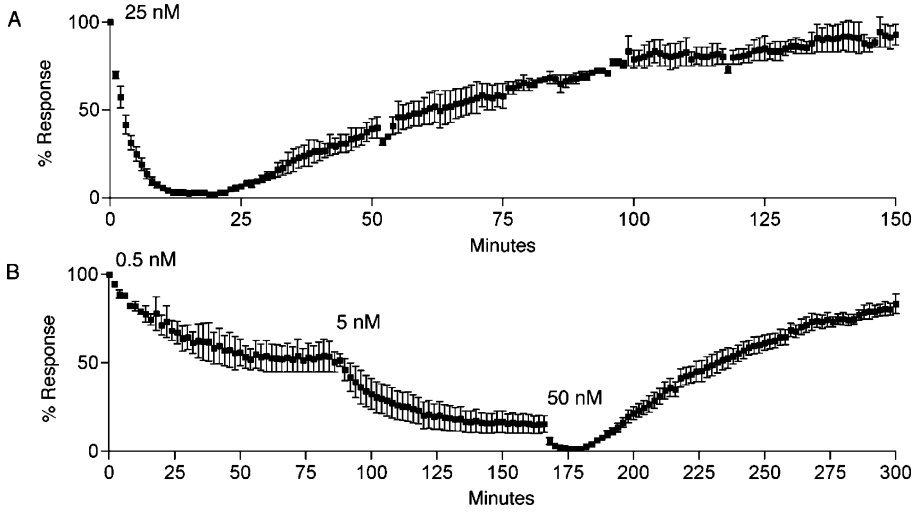

FIGURE 3: Kinetics of block and recovery of the mouse fetal muscle nAChR by αA-OIVA. Results were obtained by toxin perfusion over voltage-clamped *Xenopus* oocytes. Oocytes were pulsed with ACh once per 2 min. (A) A 25 nM concentration of αA-OIVA was perfused over oocytes expressing the mouse fetal muscle nAChR until the peak amplitude of the elicited currents reached a steady state (equilibrium block). After the peak amplitude of currents reached equilibrium, the toxin was allowed to wash out by perfusion of ND96 without toxin ($n = 3$) (B) Various concentrations of αA-OIVA were perfused over oocytes expressing the mouse fetal muscle nAChR. After each concentration reached an equilibrium block, a higher concentration of toxin was then perfused over the oocytes. After a nearly complete block, perfusion of ND96 resumed and toxin was allowed to wash out ($n = 3$). This method was used to determine the dose−response curve in Figure 1 for αA-OIVA. A k_{on} value was determined for each perfusion concentration independently. The mean and range of k_{on} values are reported below. The kinetic parameters were as follows: $k_{off} = 1.35 \times 10^{-2}$ min^{-1} ($1.19-1.50 \times 10^{-2}$ min^{-1}, 95% CI), mean $k_{on} = 2.07 \times 10^7$ M^{-1} min^{-1} (range of $7.22 \times 10^6-5.37 \times 10^7$ M^{-1} min^{-1}). K_d calculated from k_{off} and k_{on} was 0.65 nM, consistent with the ∼50% block by perfusion of 0.5 nM αA-OIVA. Given the calculated k_{off} and k_{on} values, the differences in time to reach equilibrium for 0.5 and 5 nM toxin concentrations should have been greater, indicating a degree of uncertainty in kinetic measurements.

regression analysis of toxin perfusion and wash-out data. The best curve fit of the toxin perfusion data was obtained in each case for the following equation: $y = \text{span} \times e^{-k_{obs}t} + \text{plateau}$, where span is the difference between the control response (100% response) and equilibrium % response, plateau is the equilibrium % response, k_{obs} is the rate constant obtained by the best curve fit of the current block, and t is time. The k_{on} rate constant was calculated from k_{obs} by the equation: $k_{obs} = k_{on}[\text{toxin}] + k_{off}$. The dissociation rate constant, k_{off}, was calculated with Prism software by obtaining the best fit of the toxin wash-out curve using the following equation: $y = y_{max}(1 - e^{-k_{off}t})$, where y_{max} is 100% response and t is time.

RESULTS

Cloning and Synthesis of C. pergrandis αA-Conotoxins. Two DNA sequences encoding homologues of the αA-OIVA and αA-OIVB peptides were obtained by molecular cloning from *C. pergrandis* as described in the Materials and Methods. The nucleotide sequences and predicted amino acid sequences for the mature toxins are the following (Chart 1). On the basis of the presence of hydroxyproline residues in αA-OIVA and αA-OIVB (*7*, *8*), we predicted that these sequences would also have hydroxyproline residues. Additionally, because the DNA sequences included stop codons immediately following the last Cys codon, the peptides were predicted to have free carboxyl C termini, in contrast to the amidated C termini of αA-OIVA and αA-OIVB. Each peptide was chemically synthesized with a free carboxyl C terminus and hydroxyproline residues. Only one amino acid difference was predicted between these two peptides. After their characterization, these peptides were named αA-conotoxin PeIVA (αA-PeIVA) and αA-conotoxin PeIVB (αA-PeIVB).

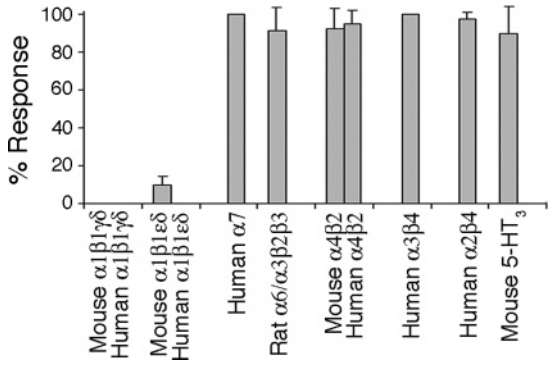

FIGURE 4: αA-Conotoxin OIVA has specificity for muscle nAChRs. *Xenopus* oocytes heterologously expressing various ligand-gated ion channels were voltage-clamped. All of the receptors indicated are subtypes of nicotinic acetylcholine receptors, with the exception of the 5-HT$_3$ receptor, which is a serotonin-gated ion channel. Each toxin−receptor combination was tested on at least two different oocytes to establish reproducibility. The bars represent the peak amplitude current response as a percentage of the control response obtained prior to the bath application of toxin (error bars = ±SEM). While 10 μM αA-OIVA was a concentration sufficient to inhibit the adult muscle nAChR, as well as the fetal muscle nAChR, αA-OIVA is selective for the fetal subtype, as demonstrated in Figure 1.

Characterization of αA-PIVA, αA-OIVA, αA-PeIVA, and αA-PeIVB. While αA-PIVA and αA-OIVA have been partially characterized (*8*, *9*), the selectivity of these peptides for mammalian fetal and adult muscle nAChRs was not previously investigated. αA-conotoxin EIVA (αA-EIVA), from *C. ermineus*, has been shown to be a high-affinity inhibitor of both fetal and adult mammalian muscle nAChRs because it competitively binds both the α/γ and α/δ interfaces of the muscle nAChR with equal affinity (*10*): the α/δ interface is present in both adult and fetal nAChR subtypes. αA-PIVA is shorter than αA-EIVA but longer than

Table 4: Summary of Short αA-Conotoxins and Dissociation Rate Kinetics from the Mouse Fetal Muscle NAChR[a]

conotoxin	k_{off} value x 10^{-2} min^{-1}	amino acid sequence
fast off rate		
αA-OIVB	70 (63−76)	**CC**GVONAA**C***P*O**C**V**C**NKT**C**G#
αA-OIVA[H10P]	79 (73−86)	**CC**G<u>V</u>ONAA**C**<u>*P*</u>O**C**V**C**<u>KNT</u>**C**#
slow off rate		
αA-OIVA	1.35 (1.19−1.50)	**CC**GVONAA**C***H*O**C**V**C**KNT**C**#
αA-OIVA[K15N]	0.43 (0.38−0.49)	**CC**G<u>V</u>ONAA**C***H*O**C**V**C**<u>NNT</u>**C**#
αA-OIVA[K15R]	<2.0	**CC**G<u>V</u>ONAA**C***H*O**C**V**C**<u>RNT</u>**C**#
αA-OIVA[K15N,N16K]	<2.0	**CC**G<u>V</u>ONAA**C***H*O**C**V**C**<u>NKT</u>**C**#
αA-PeIVA*	0.82 (0.81−0.83)	**CC**G<u>V</u>ONAA**C***H*O**C**V**C**<u>TGK</u>**C**
αA-PeIVB	<2.0	**CC**G<u>I</u>ONAA**C***H*O**C**V**C**<u>TGK</u>**C**

[a] Amino acid differences are underlined and/or italicized. Parentheses indicate the 95% CI. (*) αA-PeIVA dissociation rate calculation was based on a single experiment. All other k_{off} values were based on three or more experiments. An extended time course of dissociation was not conducted for αA-OIVA[K15R], αA-OIVA[K15N,N16K], or αA-PeIVB. O = hydroxyproline. # = amidation.

αA-OIVA and αA-OIVB (see Table 2 for a direct comparison of these sequences).

We tested αA-PIVA for its ability to discriminate between mammalian fetal and adult muscle nAChRs using two-electrode voltage clamping of *Xenopus* oocytes heterologously expressing cloned receptors, as described in the Materials and Methods. Significantly, in contrast to αA-OIVB, αA-PIVA antagonized both the mouse fetal and adult muscle nAChRs with high affinity, consistent with its greater sequence similarity to αA-EIVA (Figure 1). αA-PIVA, in contrast to αA-OIVB, had a somewhat higher affinity for the adult subtype of the receptor.

Subsequently, we tested αA-OIVA for its ability to discriminate between mammalian fetal and adult muscle nAChRs, also by oocyte electrophysiology. Toxin dose−response curves were generated for both receptor subtypes. αA-OIVA proved to be selective for the mouse fetal muscle nAChR, consistent with its similarity to αA-OIVB. Notably, αA-OIVA blocked the mouse fetal muscle nAChR with ∼600-fold greater affinity than the adult subtype (Figure 1) and also exhibited a similar affinity difference for the human fetal and adult muscle nAChRs expressed in *Xenopus* oocytes (data not shown). The αA-OIVB peptide had ∼1500-fold greater affinity for the mouse fetal muscle nAChR over the adult subtype (Figure 1), consistent with the dose−response curves previously generated for αA-OIVB on the human muscle nAChR, where αA-OIVB demonstrated ∼2000-fold greater affinity for the fetal subtype (*7*). αA-PeIVA also proved to have selectivity for the fetal muscle nAChR, consistent with its high degree of sequence similarity to αA-OIVA and αA-OIVB. The IC_{50} values of these peptides for fetal and adult nAChR subtypes are shown in Table 3.

Although αA-OIVA and αA-PeIVA, like αA-OIVB, have strong selectivity for the mouse fetal muscle nAChR subtype, they dissociate from this receptor with a much slower off rate than αA-OIVB, as shown in the electrophysiology traces in Figure 2. αA-PeIVB also dissociated very slowly from the fetal muscle nAChR (data not shown). We quantified the αA-OIVA kinetic parameters of the block of the mouse fetal muscle nAChR by perfusion of the toxin over *Xenopus* oocytes heterologously expressing the fetal receptor (Figure 3). It proved to be very difficult to quantify the kinetics because of the very slow rate of block and recovery, the limited lifetime of any given oocyte after voltage clamping, the tendency for current amplitude to drift over time, and the large quantities of toxin required for both failed and successful experiments. Kinetic parameters were determined as described in the Materials and Methods and as indicated in the caption of Figure 3. A similarly slow dissociation rate was obtained by perfusion of αA-OIVA over oocytes expressing the human fetal muscle nAChR (data not shown).

αA-OIVB was previously shown to be selective not only between the fetal and adult muscle nAChRs but was also shown to have very little affinity for neuronal nAChRs (*7*). Similarly, we also tested αA-OIVA against several other ligand-gated ion channels expressed in *Xenopus* oocytes to understand better its targeting specificity. At a concentration of 10 μM, αA-OIVA failed to significantly inhibit various ligand-gated ion channels (ref *8* and Figure 4). These experiments attest to the targeting specificity of both αA-conotoxins OIVA and OIVB for muscle nAChRs and their selectivity for the fetal subtype of the muscle nAChR.

Characterization of αA-OIVA Analogues. Analogues of αA-OIVA were synthesized and tested to assess which amino acids might contribute to the differences in dissociation kinetics from the fetal muscle nAChR for αA-OIVA and αA-OIVB demonstrated in Figure 2. The amino acid sequences of the analogues are shown in Table 4.

The αA-OIVA[K15N], αA-OIVA[K15R], and αA-OIVA-[K15N,N16K] analogues all demonstrated a very slow off rate from the fetal muscle nAChR, similar to native αA-OIVA, αA-PeIVA, and αA-PeIVB. Selected electrophysiology traces are shown in Figure 5. These peptides have divergent sequences in their C-terminal intercysteine region, and αA-PeIVA and αA-PeIVB differ from the others in having carboxylated C termini. Thus, we hypothesized that a primary determinant of the slow off rate was the shared histidine residue at position 10. A direct confirmation of this hypothesis was provided when αA-OIVA[H10P] dissociated very rapidly from the fetal muscle nAChR, similarly to αA-OIVB (Figures 2 and 5). Collectively, these results indicated that the histidine versus proline residue at position 10 is the critical amino acid difference between αA-OIVA, αA-PeIVA, αA-PeIVB, and αA-OIVB that determines the dramatically different dissociation rates from the fetal muscle nAChR. These data are summarized in Table 4.

When the histidine residue in αA-OIVA was replaced with proline, the dose−response curves of αA-OIVA[H10P] became statistically indistinguishable from the dose−response curves generated for αA-OIVB on the fetal and adult muscle nAChRs (Figure 6). This result suggested that the histidine or proline residue at position 10 determines not

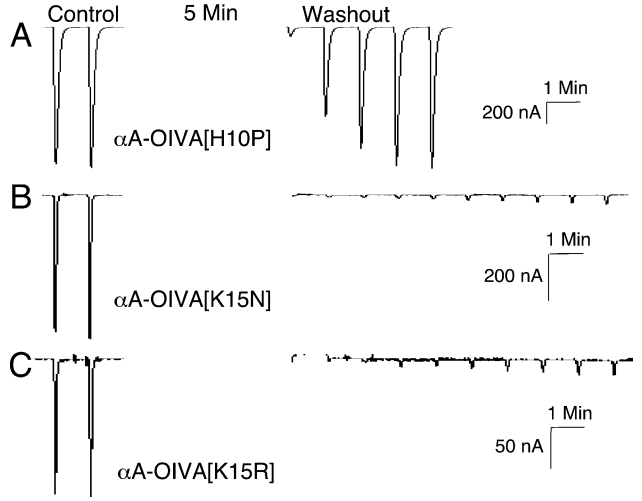

FIGURE 5: Analogues of αA-OIVA demonstrate distinct dissociation rates from the mouse fetal muscle nAChR. Representative current traces are provided that illustrate the dissociation rate differences between select αA-OIVA analogues. In each case, the mouse fetal muscle nAChR was expressed in *Xenopus* oocytes. After baseline currents were established, αA-OIVA analogues were applied to a given oocyte at 10 μM final concentration and allowed to equilibrate for 5 min. (A) αA-OIVA[H10P] analogue demonstrated a rapid dissociation rate, similar to the dissociation rate of αA-OIVB (see Figure 2). (B and C) αA-OIVA[K15N] and [K15R] analogues demonstrated very slow dissociation rates, similar to the dissociation rate of αA-OIVA (see Figure 2).

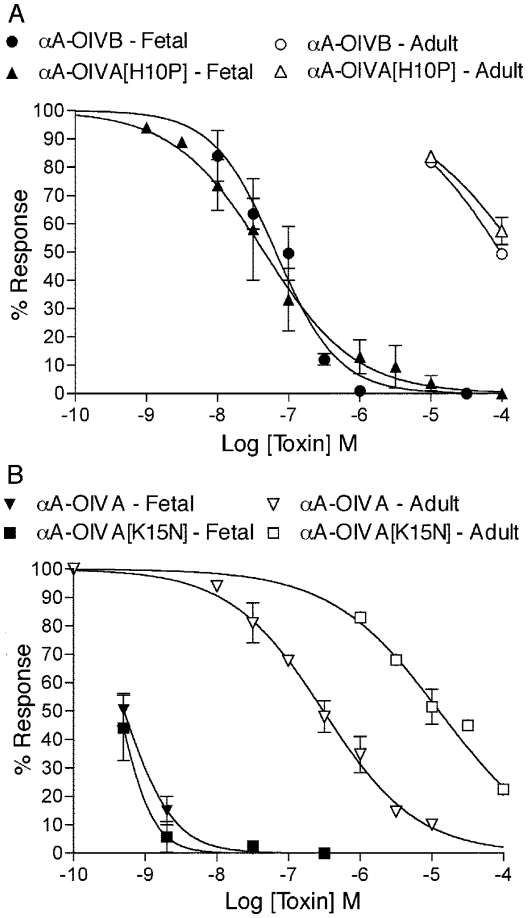

FIGURE 6: Comparison of dose−response curves generated for αA-conotoxins and analogues on mouse fetal and adult neuromuscular nAChRs. Dose−response curves were obtained from voltage-clamping *Xenopus* oocytes. (A) When the histidine at position 10 in αA-OIVA was changed to a proline residue (αA-OIVA[H10P]), the dose−response curves became statistically indistinguishable from the dose−response curves for αA-OIVB, e.g., by overlapping 95% CIs for the IC_{50} values. For the fetal subtype, the 95% CIs for the IC_{50} values were 48−92 nM for αA-OIVB and 27−74 nM for αA-OIVA[H10P]. For the adult subtype, the 95% CIs for the IC_{50} values were 81 000−110 000 nM for αA-OIVB and 74 000−300 000 nM for αA-OIVA[H10P]. (B) When the lysine at position 15 in αA-OIVA was changed to an asparagine residue (αA-OIVA-[K15N]), the dose−response curve on the fetal muscle nAChR became statistically indistinguishable from native αA-OIVA. The 95% CIs for the IC_{50} values were 0.40−0.64 nM for αA-OIVA and 0.32−0.60 nM for αA-OIVA[K15N]. However, the K15N analogue appeared to be even more selective than the native peptide for the fetal muscle nAChR. On the adult subtype, the 95% CIs for IC_{50} values were 240−390 nM for αA-OIVA and 8200−19 000 nM for αA-OIVA[K15N]. Because of the very slow kinetics of the block by αA-OIVA and αA-OIVA[K15N], only partial dose−response curves for the fetal muscle nAChR were obtained by perfusion of various concentrations of toxin over the oocytes as demonstrated in Figures 3 and 7.

only the dissociation rate differences but also the affinity differences between αA-OIVA and αA-OIVB, which is reasonable because affinity is a function of k_{on} and k_{off}. Further supporting this hypothesis, αA-OIVA[K15N] had approximately the same affinity as native αA-OIVA for the fetal muscle nAChR; surprisingly, αA-OIVA[K15N] appeared to have a lower affinity than native αA-OIVA for the adult subtype (Figure 6).

The kinetic parameters for αA-OIVA[K15N] were determined by perfusion of toxin over *Xenopus* oocytes expressing the mouse fetal muscle nAChR. αA-OIVA[K15N] unexpectedly exhibited even slower kinetics of block and recovery than native αA-OIVA (Figures 3 and 7). Because αA-OIVA-[K15N] exhibited both greater selectivity between fetal and adult muscle nAChRs and a slower dissociation rate from the fetal subtype than native αA-OIVA, the analogue may prove to be a more useful research tool than the native peptide.

DISCUSSION

In this paper, we have identified new members of the αA-conotoxin family and provided a more detailed functional definition of this conotoxin family. Cumulatively, these studies lead us to propose that the αA-conotoxin family can be subdivided into two groups: one includes αA-EIVA, αA-EIVB, and αA-PIVA, with the second group comprising αA-OIVA, αA-OIVB, αA-PeIVA, and αA-PeIVB. We designate these two divisions as the αA_L subfamily and the αA_S subfamily. The amino acid sequences of these peptides are summarized in Table 2.

While both αA-PIVA and αA-EIVA share some sequence identity with αA-OIVA and αA-OIVB, they differ significantly in their C-terminal regions. Significantly longer primary amino acid sequences are found in the αA_L peptides than in the αA_S peptides. Thus, while the αA_L peptides are high-affinity inhibitors of both the mammalian fetal and adult muscle nAChRs, we have shown that the αA_S peptides selectively antagonize the fetal subtype. These differences, as well as differences in disulfide connectivity (*8*, *9*), justify dividing αA-conotoxins into two subfamilies.

In addition to the conotoxins, many neuromuscular nAChR antagonists have been previously characterized. Notably, the waglerins, peptide toxins from the pit viper *Trimeresurus wagleri*, bind with 2000-fold higher affinity to the α/ϵ

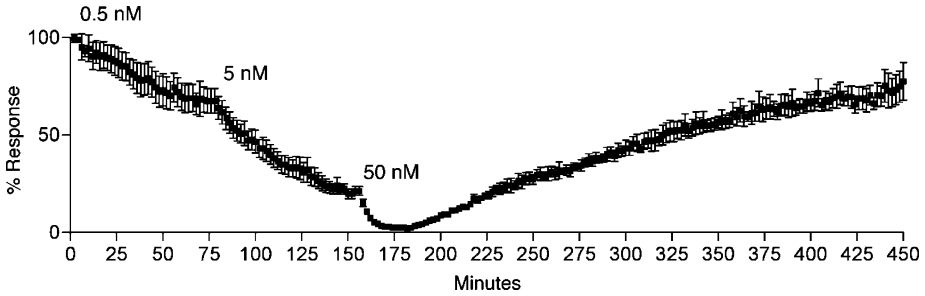

FIGURE 7: Kinetics of block and recovery of the mouse fetal muscle nAChR by αA-OIVA[K15N]. Results were obtained by toxin perfusion over voltage-clamped *Xenopus* oocytes. Oocytes were pulsed with ACh once per 2 min. Various concentrations of αA-OIVA[K15N] were perfused over oocytes expressing the mouse fetal muscle nAChR. Because of the particularly slow kinetics of the block, we did not continue perfusion of each concentration of toxin to equilibrium but were able to extrapolate the curves to plateau (equilibrium) values. These extrapolated equilibrium values were used for the partial dose−response curve for αA-OIVA[K15N] in Figure 6. After a full block of the receptors by 50 nM toxin, we resumed perfusion of ND96 and allowed toxin to wash out ($n = 4$). A k_{on} value was determined for each perfusion concentration independently. The mean and range of k_{on} values are reported below. The kinetic parameters were as follows: $k_{off} = 0.43 \times 10^{-2}$ min^{-1} ($0.38-0.49 \times 10^{-2}$ min^{-1}, 95% CI), mean $k_{on} = 7.83 \times 10^{6}$ M^{-1} min^{-1} (range of $2.86 \times 10^{6}-1.65 \times 10^{7}$ M^{-1} min^{-1}). K_d calculated from k_{off} and k_{on} was 0.55 nM, consistent with the extrapolated ∼50% block by perfusion of 0.5 nM αA-OIVA-[K15N] (see also the dose−response curve in Figure 6).

interface of the adult muscle nAChR than the α/δ and α/γ interfaces (*13*), making them selective antagonists of the adult muscle nAChR and complementary to the selectivity of the αA_S-conotoxins. Many additional snake α-neurotoxins such as α-bungarotoxin are high-affinity antagonists of both the α/δ and α/γ interfaces of the muscle nAChR. Their high-affinity block of the α/δ interface renders them nonselective for either fetal or adult receptor subtypes. An α-neurotoxin from *Naja mossambica mossambica*, known as NmmI, antagonizes both the α/δ and α/γ subunit interfaces with ∼1000-fold higher affinity than the α/ε interface (*14*). Curare and curariform antagonists bind both the α/ε and α/γ interfaces of the neuromuscular nAChR with high affinity while binding the α/δ interface with approximately 100-fold lower affinity (*15*, *16*). Some α-conotoxins bind with 10 000-fold higher affinity to the α/δ interface than the α/γ interface (*17*). As stated previously, the αA_L-conotoxin, αA-EIVA, blocks both the α/δ and α/γ interfaces with equal affinity and is consequently a high-affinity inhibitor of both fetal and adult muscle nAChRs (*10*). αA-PIVA also blocks both the adult and fetal subtypes with high affinity. Although the αA_S-conotoxins achieve their selectivity for the fetal muscle nAChR by binding the α/γ interface with much higher affinity than the α/δ or α/ε interfaces, we have not identified the αA_S-conotoxin selectivity between δ or ε subunits of the adult receptor in this study.

There is an interesting kinetic parallel *in vivo* and *in vitro* with the αA_S-conotoxins. αA-conotoxin OIVA causes an apparently irreversible paralysis upon injection into goldfish (*8*) and exhibits a very slow off rate when applied to the mammalian fetal muscle nAChR. In contrast, αA-conotoxin OIVB causes a reversible paralysis upon injection into goldfish (*7*) and exhibits rapid reversibility when applied to the mammalian fetal muscle nAChR. While little is known about fish nAChRs, the fact that the pufferfish (*Fugu*) expresses homologues of both the mammalian γ and ε subunits in mature muscle tissues may provide an evolutionary explanation for the specificity of the short αA-conotoxins (which evolved for fish hunting) for binding a mammalian fetal receptor (*7*, *18*). These toxins most likely bind to the fish receptor subunit that has the most sequence similarity to the mammalian γ subunit, found only in the mammalian fetal nAChR. The parallel kinetics suggest that enough sequence and structural similarity are conserved across vertebrate nAChRs to provide a similar kinetic profile *in vivo* and *in vitro* on homologous receptor subtypes. Neither αA-OIVA nor αA-OIVB had an observable effect on mature mice when injected at a dosage as high as 1 nmol/g, consistent with their selectivity for the mouse fetal receptor subtype (*7*, *8* and data not shown).

The selectivity of the short αA-conotoxins for the fetal muscle nAChR gives this subfamily of peptides interesting potential as research tools, diagnostic tools, and even as possible therapeutics as previously described (*7*). The diverse kinetics observed in this subfamily of peptides expand their potential as research tools; the rapidly reversible peptides would be suitable pharmacological agents for electrophysiological studies, while the slowly reversible peptides should be useful probes for binding and localization studies.

ACKNOWLEDGMENT

We thank Charleen Miller and Ron Kaiser for conducting analytical work, Dennis Winge for amino acid analysis, and Steven M. Sine for providing mouse muscle nAChR subunit clones.

REFERENCES

1. Mishina, M., Takai, T., Imoto, K., Noda, M., Takahashi, T., Numa, S., Methfessel, C., and Sakmann, B. (1986) Molecular distinction between fetal and adult forms of muscle acetylcholine receptor, *Nature 321*, 406−411.
2. Witzemann, V., Barg, B., Nishikawa, Y., Sakmann, B., and Numa, S. (1987) Differential regulation of muscle acetylcholine receptor γ- and ε-subunit mRNAs, *FEBS Lett. 223*, 104−112.
3. Witzemann, V., Barg, B., Criado, M., Stein, E., and Sakmann, B. (1989) Developmental regulation of five subunit specific mRNAs encoding acetylcholine receptor subunits in rat muscle, *FEBS Lett. 242*, 419−424.
4. Nirthanan, S., and Gwee, C. E. (2004) Three-finger α-neurotoxins and the nicotinic acetylcholine receptor, 40 years on, *J. Pharmacol. Sci. 94*, 1−17.
5. Terlau, H., and Olivera, B. M. (2004) *Conus* venoms: A rich source of novel ion channel-targeted peptides, *Physiol. Rev. 84*, 41−68.
6. Olivera, B. M. (1997) E. E. Just lecture, 1996. *Conus* venom peptides, receptor and ion channel targets, and drug design: 50 million years of neuropharmacology, *Mol. Biol. Cell 8*, 2101−2109.

7. Teichert, R. W., Rivier, J., Torres, J., Dykert, J., Miller, C., and Olivera, B. M. (2005) A uniquely selective inhibitor of the mammalian fetal neuromuscular nicotinic acetylcholine receptor, *J. Neurosci. 25*, 732−736.
8. Teichert, R. W., Rivier, J., Dykert, J., Cervini, L., Gulyas, J., Bulaj, G., Ellison, M., and Olivera, B. M. (2004) αA-Conotoxin OIVA defines a new αA-conotoxin subfamily of nicotinic acetylcholine receptor inhibitors, *Toxicon 44*, 207−214.
9. Hopkins, C., Grilley, M., Miller, C., Shon, K. J., Cruz, L. J., Gray, W. R., Dykert, J., Rivier, J., Yoshikami, D., and Olivera, B. M. (1995) A new family of *Conus* peptides targeted to the nicotinic acetylcholine receptor, *J. Biol. Chem. 270*, 22361−22367.
10. Jacobsen, R., Yoshikami, D., Ellison, M., Martinez, J., Gray, W. R., Cartier, G. E., Shon, K. J., Groebe, D. R., Abramson, S. N., Olivera, B. M., and McIntosh, J. M. (1997) Differential targeting of nicotinic acetylcholine receptors by novel αA-conotoxins, *J. Biol. Chem. 272*, 22531−22537.
11. Volkovsky, T. (1995) Detection of secondary amines on solid phase, *Pept. Res. 8*, 236−237.
12. Cartier, G. E., Yoshikami, D., Gray, W. R., Luo, S., Olivera, B. M., and McIntosh, J. M. (1996) A new α-conotoxin which targets α3β2 nicotinic acetylcholine receptors, *J. Biol. Chem. 271*, 7522−7528.
13. McArdle, J. J., Lentz, T. L., Witzemann, V., Schwarz, H., Weinstein, S. A., and Schmidt, J. J. (1999) Waglerin-1 selectively blocks the ϵ form of the muscle nicotinic acetylcholine receptor, *J. Pharmacol. Exp. Ther. 289*, 543−550.
14. Osaka, H., Malany, S., Kanter, J. R., Sine, S. M., and Taylor, P. (1999) Subunit interface selectivity of the α-neurotoxins for the nicotinic acetylcholine receptor, *J. Biol. Chem. 274*, 9581−9586.
15. Sine, S. M. (1993) Molecular dissection of subunit interfaces in the acetylcholine receptor: Identification of residues that determine curare selectivity, *Proc. Natl. Acad. Sci. U.S.A. 90*, 9436−9440.
16. Bren, N., and Sine, S. M. (1997) Identification of residues in the adult nicotinic acetylcholine receptor that confer selectivity for curariform antagonists, *J. Biol. Chem. 272*, 30793−30798.
17. Groebe, D. R., Dumm, J. M., Levitan, E. S., and Abramson, S. N. (1995) α-Conotoxins selectively inhibit one of the two acetylcholine binding sites of nicotinic receptors, *Mol. Pharmacol. 48*, 105−111.
18. Jones, A. K., Elgar, G., and Sattelle, D. B. (2003) The nicotinic acetylcholine receptor gene family of the pufferfish, *Fugu rubripes*, *Genomics 82*, 441−451.

BI052016D